Progress In Electromagnetics Research M, Vol. 73, 153–162, 2018

Low Loss High Power Air Suspended Stripline Power Divider for High Power Division Sub-Systems Applications

Ahmed F. Elshafey and Mahmoud A. Abdalla*

Abstract—In this paper, a high power, air suspended stripline (SSL) T junction power divider at L band microwave frequencies is introduced. The power divider operating frequency is centered at 1.3 GHz. In this new configuration, the only dielectric used is air to have maximum power handling capability. An excitation transition from coaxial cable to the SSL transmission line is explained. The SSL was fabricated using aluminum sheets to gain the advantage of low cost. The power divider design was validated using circuit and 3D full wave simulations and confirmed using experimental measurements with all agreements. It has been proved that the power divider attenuation has sharp rejection characteristic at the designed frequency (−20 dB at 1.3 GHz). The power divider can be used as a feeder for devices used in high power applications.

1. INTRODUCTION

The increased need for high power microwave components has become essential in modern communication, radars and satellite systems [1]. Power divider is one of the most basic high-power components which are widely used in high power circuits and systems, such as antennas [2–4] amplifiers [5, 6], six-port circuits [7], push-pull circuits [8].

The two power divider architectures are T-junction and the Wilkinson power divider. Wilkinson power divider has the advantage of isolation between and matched at all ports [9–14]. However, using lumped elements to isolate between the output ports makes it bulky. On the other hand, T-junction is simpler and more compact than Wilkinson power divider which makes it suitable for L band microwave applications. However, it is worth to comment that T junction has no isolation between the output ports and is not matched at all ports which need carefulness in the design. T-junction can be formed in the form of microstrip or stripline configuration [15–18].

High power applications suffer from increasing losses (ohmic loss and dielectric losses) that may exist in planar transmission lines (as microstrip lines). One of the solutions of this problem is using suspended stripline (SSL) [19]. In the (SSL) the center conductor is printed on a substrate which is suspended between two parallel ground plates which reduce the losses compared to microstrip configuration [20]. SSL configuration is used to support the high power due to its low insertion loss and high-power handling capability. However, SSL configuration still has losses due to multi-dielectrics losses in which the strip conductor is printed [21–23].

In this paper, a new, SSL transmission line using an air substrate to handle high power is introduced. The transition from coaxial cable to the SSL is investigated in Section 2. Based on the SSL, a three-way low loss, low cost and high power (up to 15 KW) power divider is introduced. The presented results are supported by 3D full wave simulations (employing the commercial software Computer Simulation Technology (CST) and practical measurements as will be illustrated in Section 3.

Received 5 July 2018, Accepted 6 September 2018, Scheduled 22 September 2018

* Corresponding author: Mahmoud Abdelrahman Abdalla (maaabdalla@ieee.org).

The authors are with the Electromagnetic Waves Group, Electronic Engineering Department, Military Technical College (MTC), Cairo, Egypt.

2. THE SUSPENDED STRIP LINE TRANSMISSION LINE STRUCTURE

The 3D geometry of SSL transmission line is shown in Fig. 1. As shown in the figure, the structure has a middle SSL sandwiched between two air regions within which the electromagnetic waves propagate. The walls of the SSL structure are fabricated using aluminum sheets which is suitable for low cost. The used air dielectric can also handle electric field breakdown up to 3×10^6 v/m which has the advantages of low losses and high-power handling capabilities.

One of the major problems facing the guiding structures is limited ability of the transition from the coaxial lines. So, in this section we introduce the transition from coaxial cable to SSL TL over the frequency band (0 GHz to 5 GHz). Typical (ideal) SSL TL is shown in Fig. 2(a) where the SSL TL has two conductor sides. These two-sided walls were added to avoid the radiated losses. Ideal exciting of the SSL TL can be done using an infinite waveguide whose aperture coincides with the SLL TL ends. A depiction for this ideal excitation is shown in Fig. 2(b) employing waveport excitation in commercial software ANSYS-Electronic Desktop. The simulated scattering parameter magnitudes for this configuration are shown in Fig. 3. As shown in the figure, the excitation has a transmission coefficient $(S_{21}) = 0$ dB and an average reflection coefficient $(S_{11}) - 70$ dB over the frequency band 1 GHz–5 GHz. These levels will be used as a reference target for practical transition.

The excitation for the SSL TL has been designed using coaxial cable transition as shown in Fig. 4. The transition was designed as a hole inside the SSL TL end with probe coming from the inner conductor of the coaxial cable taking into consideration that the upper and lower metal sheets are hidden to illustrate the internal details of the structure. However, the ground connection of the transition is clearer in Fig. 1. In practical measurement, this coaxial cable is used as N type with the following specifications (1) The connector is 50 Ω. (2) The coaxial inner and outer conductors are made from Nickel to support high power. (3) The inner conductor is plated with gold to decrease losses. The high-power N connector has two walls of thickness = 8 mm to support the connector (of thickness = 4 mm). The simulated electric field distribution over the transition at 2.5 GHz is shown in Fig. 5. It is obvious

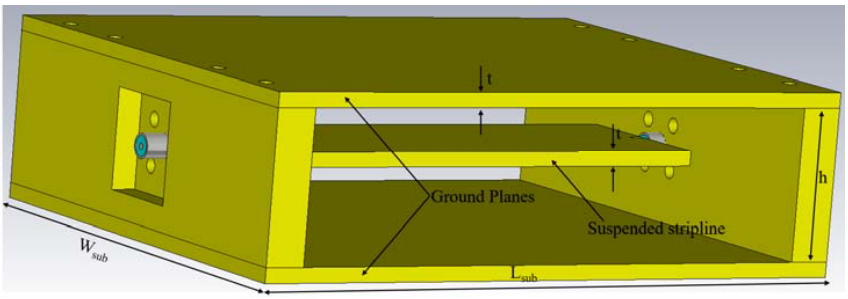

Figure 1. Completely 3D geometry of SSL transmission line.

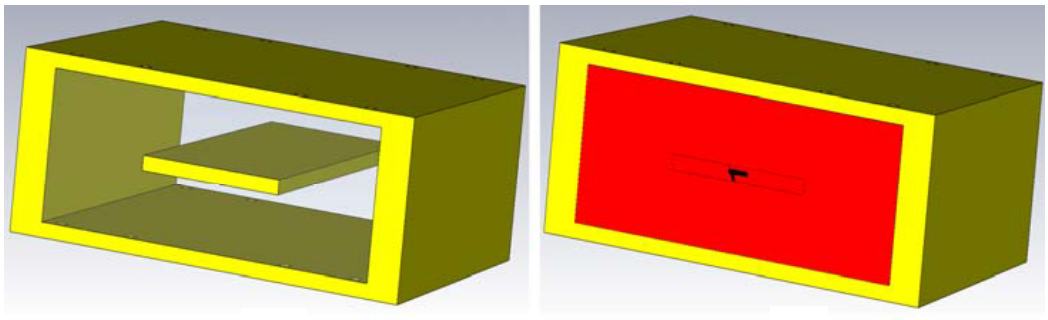

(a) (b)

Figure 2. (a) The 3D geometry for the SSL transmission line with two side walls, (b) the waveguide wave port excitation.

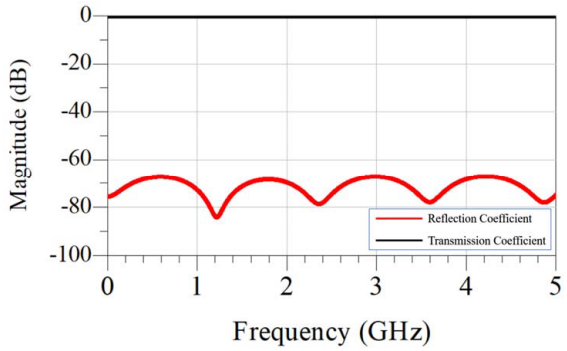

Figure 3. The ideal simulated S-parameters magnitudes of the SSL transmission line (with waveguide waveport).

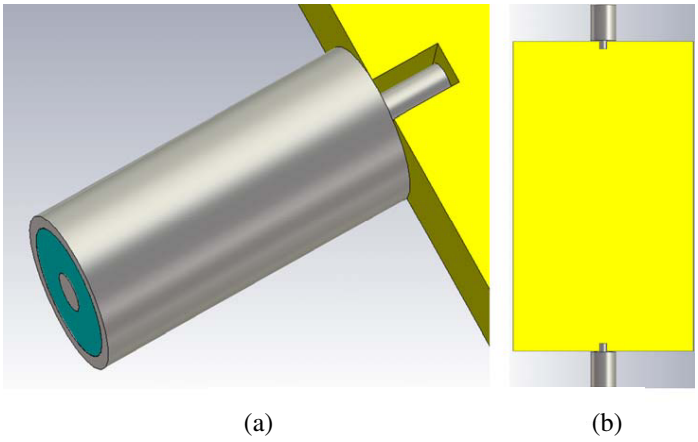

Figure 4. Single coaxial cable to SSL transition, (a) side view of the transition, (b) top view.

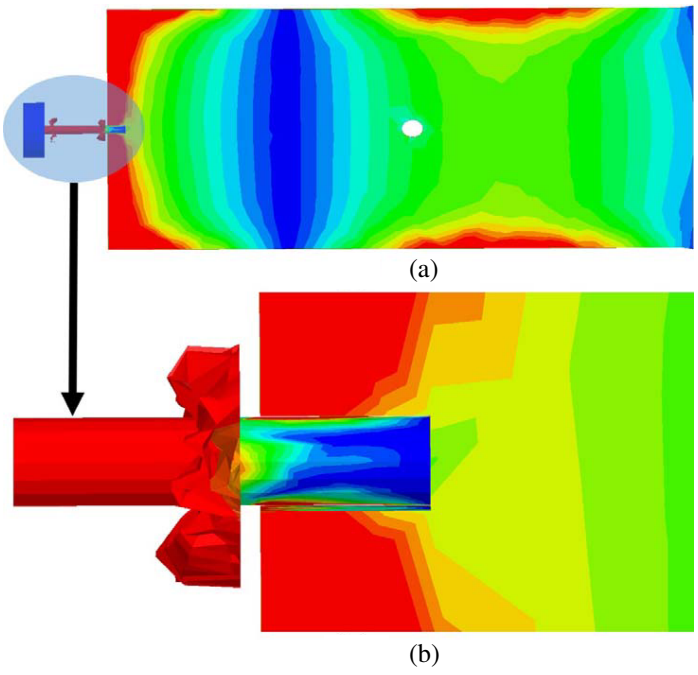

Figure 5. (a) Coaxial to stripline transition at 2.5 GHz, (b) zooming at the input probe to indicate the transition.

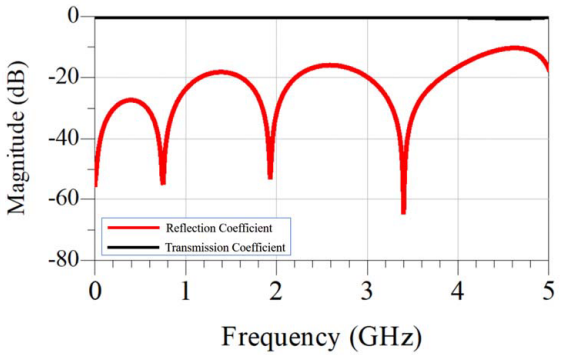

Figure 6. Simulated S-parameters of the transition from coaxial line to SSL transmission line.

that the maximum filed within the RF connector is transitioned with the same maximum distribution inside the SSL TL.

In quantitative representation of the transition success, the simulated scattering parameters of the transition are plotted in Fig. 6. As shown in the figure, the transmission coefficient (S_{21}) is almost 0 dB whereas the reflection coefficient (S_{11}) is better than -20 dB over the band from 0 to 3.9 GHz, and it increases to -15 dB from 3.9 GHz to 5 GHz. Comparing results in Fig. 3 and Fig. 6, it can be claimed that the proposed transition is successful for power transfer with acceptable matching properties over the frequency band of interest.

From another point of view, to analyze the propagated mode inside the SSL TL, a plot for the electric field and magnetic field distributions inside the SSL TL at 2.5 GHz is shown in Fig. 7. It is obvious that the electric field is radial outside the inner strip whereas the magnetic field is circulating in the direction of propagation. This means that the mode is the propagated mode as quasi TEM.

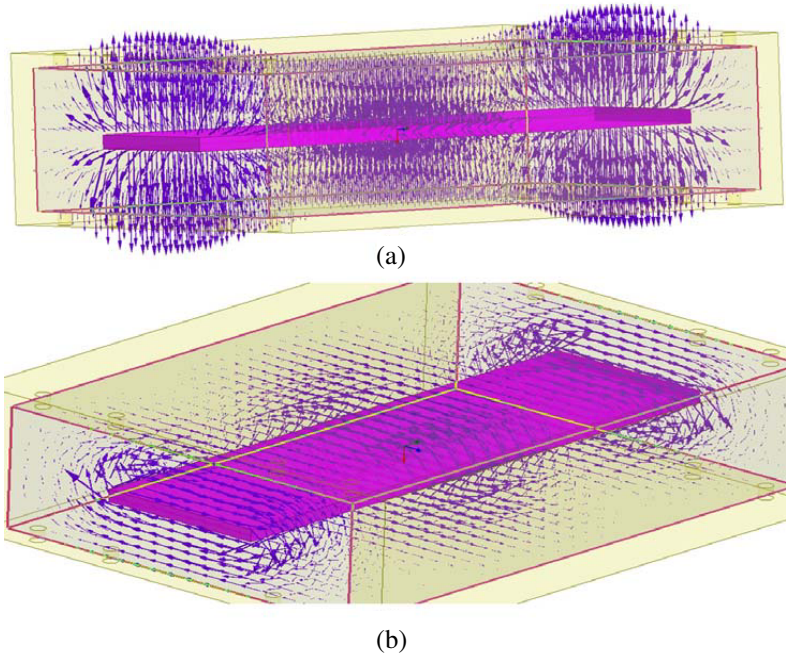

(a)

(b)

Figure 7. Field distribution inside the SSL at 2.5 GHz, (a) electric field distribution inside the suspended stripline structure, (b) magnetic field intensity inside the suspended strip line structure.

3. THE SUSPENDED STRIP LINE POWER DIVIDER

3.1. Design of the SSL Power Divider

The SSL power divider specifications are tabulated in Table 1.

Table 1. Specifications of the high power (SSL) power divider.

Operating frequency	1.3 GHz
Bandwidth of operation	0 GHz–1.55 GHz
Reflection coefficient	Up to −20 dB
Transmission coefficient	−3 dB equally division
VSWR	< 2
Power Handling Capability	Up to 15 KW (continuous Wave (C.W))

The 3D geometry structure of the SSL power divider is shown in Fig. 8(a) whereas its 2D suspended (center) divider layout is shown in Fig. 8(b). The power divider design is based on making the center divider suspended between the two ground plates without the need of any dielectric to print the divider on. Air is used as the dielectric to support the high power because of its high-power handling capability due to its high breakdown voltage. The fabricated power divider prototype is shown in Fig. 9. The power divider is fed by a 50 Ω N type feeder that is soldiered to the suspended line.

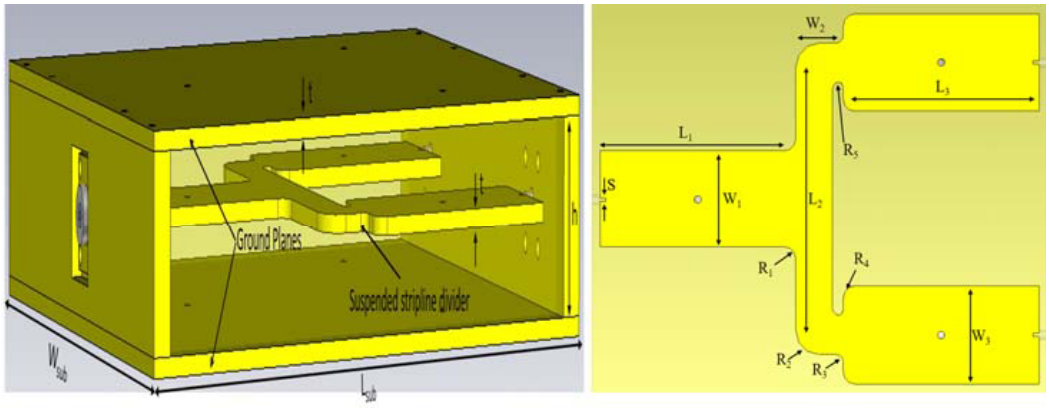

(a) (b)

Figure 8. The suspended stripline power divider, (a) 3D geometry, (b) the 2D layout of suspended stripline power divider.

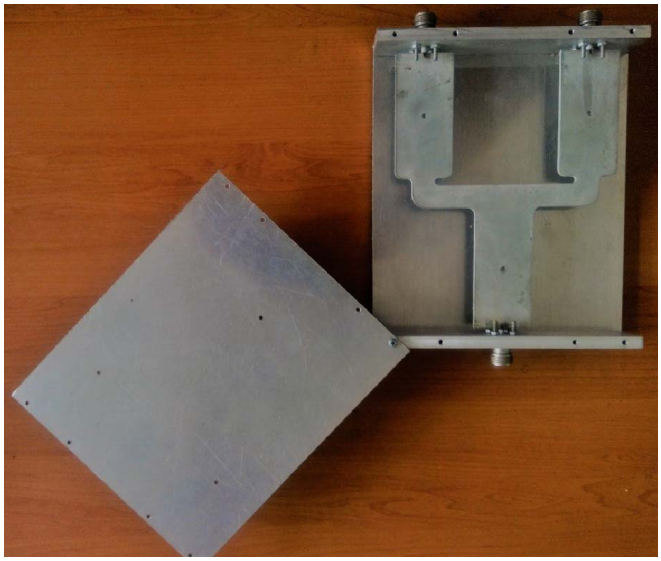

Figure 9. The fabricated suspended stripline power divider prototype.

The divider consists of an input line which is 50 Ω and is matched with the N type feeder. Then the power is divided equally between the two output lines which are also 50 Ω. Two $\lambda/4$ transformers are 70.7 Ω, and they are used to have a 50 Ω output system T junction at output ports. To reduce the losses resulting from the sharp edges, SSL discontinuities have been curved to avoid the accumulation of the voltage at these sharp edges. The power divider is fabricated from aluminum sheets of different thickness to become compatible with the available fabrication facilities and for achieving minimum loss and maximum power handling along with low cost. The detailed dimensions are tabulated in Table 2.

3.2. Results of the SSL Power Divider

The designed SSL power divider was simulated with CST. It is worth to comment that the SSL power divider layout discontinuities have been formed in curved shapes to avoid power losses at sharp edges. The simulated and measured reflection coefficients at the feeding input (S_{11}) and transmission coefficient (S_{21}) of the designed SSL power divider are shown in Fig. 10. Also, the reflection coefficient at output ports (S_{22}) with another transmission coefficient is shown in Fig. 11(a) whereas the isolation scattering parameter (S_{32}) between the output ports is shown in Fig. 11(b). As shown in the two figures, within the

Table 2. Dimensions of the SSL power divider.

Parameters and Dimensions (mm)					
Parameter	L_{sub}	W_{sub}	L_1	L_2	W_1
Dimension	214.2	180	80	108	40
Parameter	W_2	h	t	s	R_1
Dimension	15.9	30	3	1.4	5
Parameter	R_2	R_3	R_4	R_5	W_3
Dimension	10	3	5	3	40

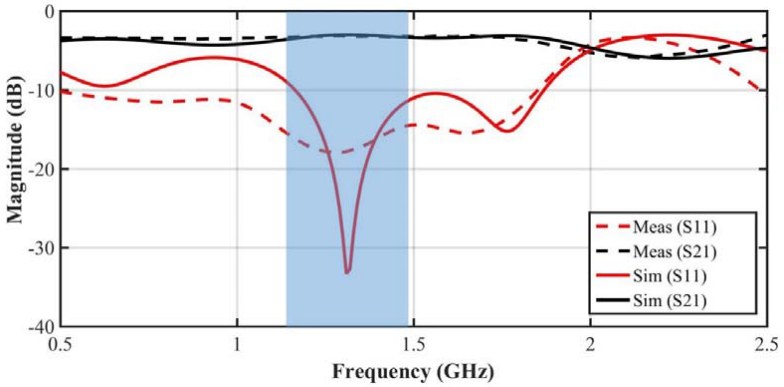

Figure 10. The simulated and measured scattering parameters magntiudes of the suspended stripline power divider.

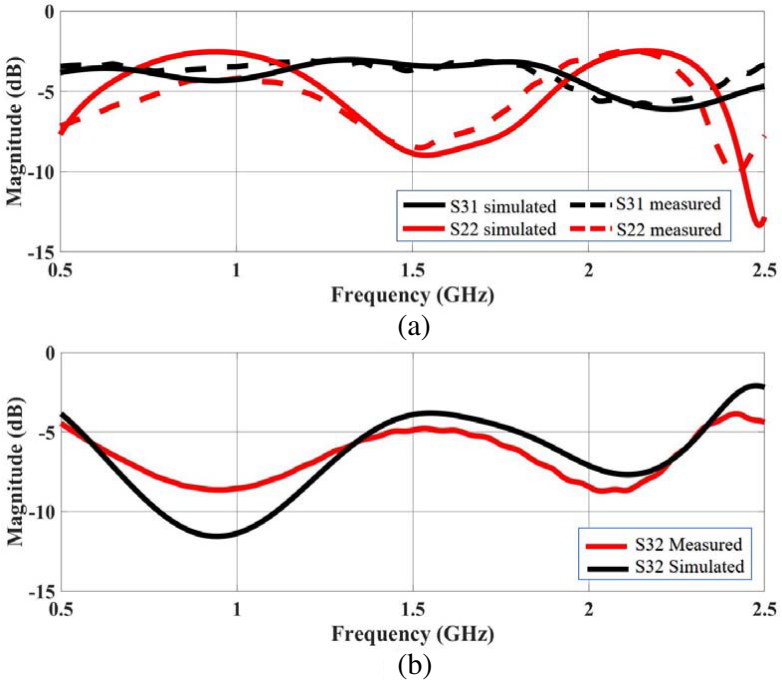

Figure 11. The other scatering parameters (a) the simulated and measured S_{22} and S_{31} of the simulated and measured isolation parameter S_{32} of the suspended stripline power divider.

desired bandwidth, the output power is equally divided at the two output ports (S_{21} and $S_{31} = -3\,\text{dB}$), and the input port is well matched (S_{11} is less than $-10\,\text{dB}$). It is also clear that there is a resonance in S_{11} curve at 1.3 GHz (design frequency) at which its values is less than $-30\,\text{dB}$ in simulation and close to $-20\,\text{dB}$ in measurements. On the other hand, the isolation between the two output ports is at its typical value of the T Junction ($S_{32} = -6\,\text{dB}$). This is also achieved for a typical value for the matching at output port ($S_{22} = -6\,\text{dB}$) at the designed frequency. In general, the measurement provides good agreement with the simulation results.

To examine the matching properties from another sensitive results demonstration, the proposed SSL power divider VSWR at input port for simulated and measured results are plotted in Fig. 12. As shown in the figure, the maximum VSWR is less than 2 within the frequency band of interest. It goes to almost 1 at design frequency (1.3 GHz).

Finally, the simulated electric field profiles through the SLL power divider structure animation of SSL power divider at 1.3 GHz is shown in Fig. 13. This figure demonstrates the in-phase equal power division at the output ports of the SSL junction at the two output ports.

To judge the SSL power divider power handling, it was tested by field test measurements. The measurements confirm that it can withstand up to 15 KW with continuous wave (C.W) input.

The power handling capability of SSL power divider can be calculated as in Eq. (1) [24–26]

$$P_{\max} = \frac{1}{2}\frac{V_{0\max}^2}{Z_0} \tag{1}$$

where $V_{o\max}$ is the maximum voltage between the line and ground, and Z_0 is the SSL line characteristic impedance $= 50\,\Omega$. According to [24–26], it is found that the stripline power divider supports up to a few KW which is compatible with SSL power divider power measurements (15 KW). So, the SSL power divider can be used in high power application.

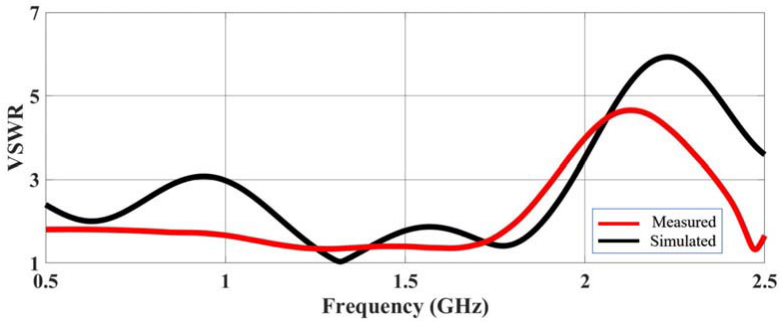

Figure 12. The VSWR at the input port of the SSL power divider.

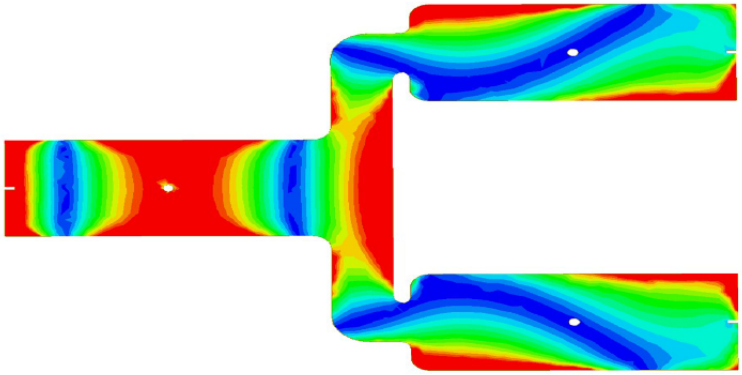

Figure 13. The electric field propagation through SSL power divider at 1.3 GHz.

Finally, to demonstrate the advantage of the proposed SSL power divider, a comparison with conventional T junction wave-guide (H plane) has been done. A standard conventional T junction waveguide (WR-650 (165.1 mm × 82.55 mm)) has been chosen to cover the L band which includes the operating frequency of interest. The waveguide T junction is illustrated in Fig. 14(a), and the simulated full wave scattering parameters are plotted in Fig. 14(b). As shown in the figure, it is clear that there is an equal power division between the output ports within the desired band ($S_{21} = S_{31} = -4.3$ dB) with reasonably good matching (S_{11} is below -10 dB) within the frequency band (1.2 GHz–1.6 GHz).

Also, the theoretical power handling capability of an air filled WR-650 waveguide has been

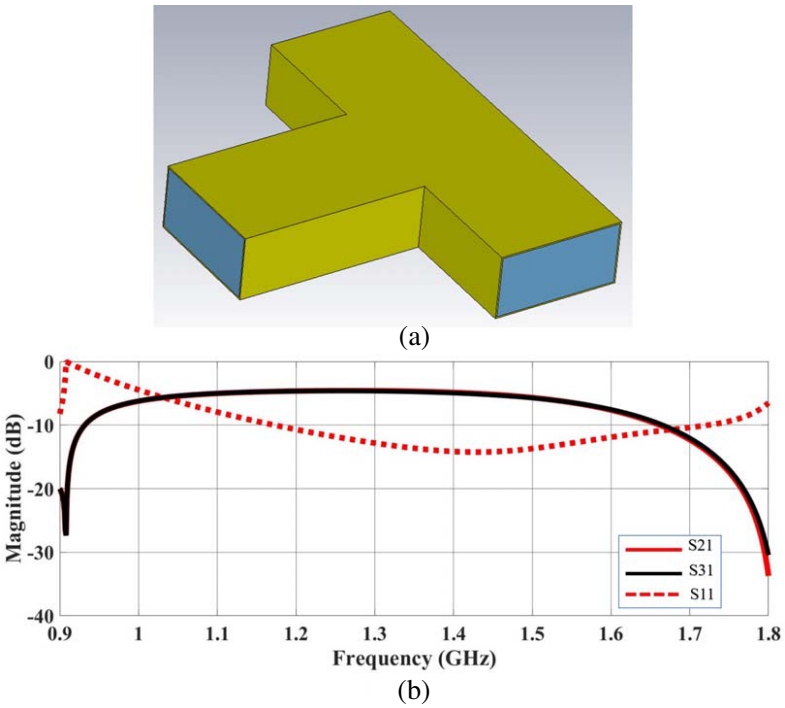

Figure 14. (a) 3D geometry of the conventional T junction waveguide power divider at L band, (b) the simulated scatering parameters magnitudes of the conventional waveguide power divider.

Table 3. A comparsion with the proposed SSL power divider and the T junction waveguide power divider.

Property	SSL Power Divider	Conventional T junction (WR-650) waveguide power divider (H section)
Size	Simpler than the T junction waveguide power divider	More complex than the SSL power divider
Transmission coefficient	−3 dB equally division	−4.3 dB equally division
Reflection coefficient	Up to −20 dB	Less than −10 dB, Up to −13 dB
Power Handling Capability	Few KW (theoretical), Up to 15 KW (C.W) measured	Up to 81 MW (theoretical)
Bandwidth of operation	0 GHz–1.55 GHz	1.2 GHz–1.6 GHz
Fabrication	Easy to fabricate	Difficult in fabrication
VSWR	< 2	> 2
Mode of propagation	TEM	TE_{10}

calculated as in Eq. (2) [27]

$$P_{\max} = \frac{1}{4}\frac{E_{\max}^2 ab}{\eta_o} \tag{2}$$

where, $E_{\max}$ is the air breakdown field = 3 Mv/m; a and b are the inside dimensions of the WR-650 waveguide; η_0 is the air intrinsic impedance = 377 Ω. Hence it has been calculated to be $P_{\max} = 81$ MW.

Finally, a comparison between the proposed SSL power divider and a conventional T junction waveguide power divider (H plane) is shown in Table 3.

4. CONCLUSION

A low loss, high power air suspended equally stripline power divider used for high power array antenna system at 1.3 GHz is presented. Air was used as dielectric without the need of other dielectrics to support high power because of its high breakdown voltage. The transition between the coaxial cable and the SSL transmission line is presented. The presented SSL power divider can support approximately up to 15 KW (C.W) and be matched at the input port (VSWR = 1). So, this configuration can be applied in designing high-power components and devices. The presented results are addressed in full wave simulation and fabricated prototypes.

REFERENCES

1. Thumm, M. K. and W. Kasparek, "Passive high-power microwave components," *IEEE Trans. Plasma Science*, Vol. 30, No. 3, 755–786, Jun. 2002.
2. Cheon, Y. and Y. Kim, "Stripline-fed aperture-coupled patch array antenna with reduced sidelobe," *Electronics Letters*, Vol. 51, No. 18, 1402–1403, Aug. 2015.
3. Czawka, G. and N. Litwinczuk, "Six-channel broadband inhomogeneous microstrip power divider for communication antenna array," *15th International Conference on Microwaves, Radar and Wireless Communications, 2004. MIKON-2004*, Vol. 3, 1020–1023, IEEE, 2004.
4. Linner, L. P. and G. Andersson, "Multi-terminal power dividers combining cavity and stripline technique," *13th European Microwave Conference, 1983*, 348–353, IEEE, Sep. 1983.
5. Nick, M. and A. Mortazawi, "A Doherty power amplifier with extended resonance power divider for linearity improvement," *2008 IEEE MTT-S International Microwave Symposium Digest*, 423–426, IEEE, Jun. 2008.
6. Riemer, P. J., J. S. Humble, J. F. Prairie, J. D. Coker, B. A. Randall, B. K. Gilbert, and E. S. Daniel, "Ka-band SiGe HBT power amplifier for single-chip T/R module applications," *IEEE/MTT-S International Microwave Symposium, 2007*, 1071–1074, IEEE, Jun. 2007.
7. Bialkowski, M. E., A. M. Abbosh, and N. Seman, "Compact microwave six-port vector voltmeters for ultra-wideband applications," *IEEE Transactions on Microwave Theory and Techniques*, Vol. 55, No. 10, 2216–2223, 2007.
8. Chiu, L., T. Y. Yum, Q. Xue, and C. H. Chan, "A wideband compact parallel-strip 180/spl deg/Wilkinson power divider for push-pull circuitries," *IEEE Microwave and Wireless Components Letters*, Vol. 16, No. 1, 49–51, 2006.
9. Sodano, H. A., "Active and passive smart structures and integrated systems," *SPIE*, Vol. 8341, 778, Mar. 2012.
10. Lee, T. H., *Planar Microwave Engineering: A Practical Guide to Theory, Measurement, and Circuits*, Vol. 1, Cambridge University Press, 2004.
11. Kao, J. C., Z. M. Tsai, K. Y. Lin, and H. Wang, "A modified Wilkinson power divider with isolation bandwidth improvement," *IEEE Transactions on Microwave Theory and Techniques*, Vol. 60, No. 9, 2768–2780, 2012.
12. Souid, B. and S. Arvas, "Yield analysis of a stripline Wilkinson power divider using Monte Carlo samples of interpolated full wave simulation data using Sonnet," *General Assembly and Scientific Symposium, 2011 XXXth URSI*, 1–4, IEEE, Aug. 2011.

13. Hirota, A., Y. Tahara, H. Yukawa, T. Owada, Y. Yamaguchi, and H. Miyashita, "A stripline power divider with insensitive to resistance variations using a parallel resistor pair," *2014 IEEE MTT-S International Microwave Symposium (IMS)*, 1–3, IEEE, Jun. 2014.
14. Tang, W., P. Zhou, X. Chen, and Y. L. Chow, "Design and optimization of stripline passive components with trust-region aggressive space mapping," *Asia-Pacific Microwave Conference, 2007. APMC 2007*, 1–4, IEEE, Dec. 2007.
15. Darwish, A. M., A. A. Ibrahim, J. Qiu, E. Viveiros, and H. A. Hung, "Novel Ka-band 'offset-divider/combiner' with reflection cancellation," *2014 IEEE MTT-S International Microwave Symposium (IMS)*, 1–3, IEEE, Jun. 2014.
16. Marki, C. F., V. D. Kodwani, and F. A. Marki, "A novel multi-octave differential power divider," *2010 IEEE MTT-S International Microwave Symposium Digest (MTT)*, 1548–1551, IEEE, May 2010.
17. Zhang, Y., Z. Wang, and R. Xu, "A Ka-band high isolation and in phase planar six way power divider based on LTCC technology," *2011 IEEE International Conference on Signal Processing, Communications and Computing (ICSPCC)*, 1–4, IEEE, Sep. 2011.
18. Grindrod, D. K., R. S. Orton, G. P. Steele, and A. J. Scammell, "Performance enhancement of TEM power dividers," *19th European Microwave Conference, 1989*, 1123–1130, IEEE, Sep. 1989.
19. Maloratsky, L. G. and R. Collins, "Reviewing the basics of suspended striplines," *Microwave Journal*, Vol. 45, No. 10, 82, Oct. 2002.
20. Zürcher, J. F., R. Głogowski, and J. R. Mosigt, "A new power divider architecture for suspended strip line," *2012 6th European Conference on Antennas and Propagation (EUCAP)*, 418–422, IEEE, Mar. 2012.
21. Kim, I. B., K. H. Kwon, S. B. Kwon, W. Mohyuddin, H. C. Choi, and K. W. Kim, "Ultra-wideband multi-section power divider on suspended stripline," *2017 IEEE MTT-S International Microwave Symposium (IMS)*, 427–430, IEEE, Jun. 2017.
22. Zhang, W., Z. Ning, Y. Wu, C. Yu, S. Li, and Y. Liu, "Dual-band out-of-phase power divider with impedance transformation and wide frequency ratio," *IEEE Microwave and Wireless Components Letters*, Vol. 25, No. 12, 787–789, 2015.
23. Fan, F. F. and Z. H. Yan, "Out-of-phase unequal power divider based on parallel dual-lines structure," *2012 International Conference on Microwave and Millimeter Wave Technology (ICMMT)*, Vol. 5, 1–3, IEEE, May 2012.
24. Bhat, B. and S. K. Koul, *Stripline-like Transmission Lines for Microwave Integrated Circuits*, New Age International, 1989.
25. Howe, H., *Stripline Circuit Design*, 102–110, Artech House, Dedham, MA, 1974.
26. Bahl, I. J. and R. Garg, "A Designer's guide to stripline circuits," *Microwaves*, 90–96, Jan. 1978.
27. Pozar, D. M., *Microwave Engineering*, John Wiley & Sons, 2009.